**Proceedings of the 2024 14th International Pipeline Conference**
**IPC2024**
**September 23-27, 2024, Calgary, Alberta, Canada**

**IPC2024-133055**

# DEVELOPMENT OF A LASER TRACKING SYSTEM BASED AI FOR AUTOMATIC ROOT PASS WELDING IN PIPES

**Daniel Galeazzi**
UFSC
Florianópolis, SC

**Régis Henrique Gonçalves e Silva**
UFSC
Florianópolis, SC

## ABSTRACT

*Today, the demands for sustainability, safety, productivity, and quality are pressing production systems, and the industry is sparing no effort to meet them. This paradigm shift towards digitalization, automation, and interconnectivity is crucial for developing smarter, more efficient manufacturing processes, in the scope of trend scenarios of Advanced Manufacturing or Industry 4.0. In this context, robotics and AI offer great solutions, that can benefit pipeline construction projects. The very viability of the new pipelines projects is affected by productivity and costs. Also, there is a strong correlation between pipeline construction and environmental issues, as well as with worker (welder) safety issues. This paper focuses on developing an AI-based laser tracking system for root pass welding in pipes, utilizing a controlled short-circuiting GMAW technology. The study employed a dedicated 7-axis anthropomorphic robot integrated with a laser sensor. The primary goal was to develop a robust integration between the robot and the laser sensor, enabling the creation of a weld seam tracking algorithm to locate and adjust the torch path along the welding of the joint. This algorithm utilized tracking points, which describe the inflection points of a previously set groove geometry. Additionally, the laser sensor system provides joint dimension data, such as bottom and top width, height, and area, which are input into an AI system to adjust welding parameters in real-time (Adaptive Welding). The AI algorithm was trained with welding parameters from experiments varying root openings and welding positions. For each condition, parameters like the controlled short-circuit current waveform, wire feed speed, travel speed, and waving parameters were optimized. Final tests were conducted on pipe sections with a V-joint to evaluate the performance and system's robustness for both algorithms path and weld parameters correction. The results demonstrated satisfactory performance: the path correction algorithm was robust, the system was capable to overcome significant geometrical variations of the root opening (1 to 4.5 mm) and pipe mismatch, and the AI algorithm performed well even in out-of-position welding, providing robustness and adequate quality to the root pass.*

Keywords: Orbital welding, Machine Learning, Online trajectory control, Smart Manufacturing, Adaptive Welding Systems.

## NOMENCLATURE

| | |
|---|---|
| AWP | Adaptive welding platform |
| RG | Root opening (mm) |
| Amp. | Amplitude (mm) |
| Freq. | Oscillation frequency (Hz) |
| ST | Stop time (ms) |
| TS | Travel Speed (cm/min) |
| I | Mean current (A) |
| WFS | Wire feed speed (m/min) |
| SP | Sample |
| CW | Clockwise |
| CCW | Counterclockwise |

## 1. INTRODUCTION

The growing demand for fossil fuels has led to an increased need for their production and distribution, sparking interest in advancements in pipeline construction. These investments translate into the creation of new pipelines and maintenance of existing ones to achieve better quality and shorter construction times, as for the need to improve current manufacturing processes. Jeff [1] noted that one of the bottlenecks in the assembly of pipelines is the welding process, which can be carried out manually, semi-automated and automated process. To increase the productivity in such operations, arc welding processes, with their higher portability, lower cost and larger weld pool [2] and thus higher robustness against joint preparation and misalignments (often found in field pipeline applications), are still the preferred welding processes.

Commercial solutions for the automation of orbital welding present a tendency to improve the welding productivity. However, constant monitoring and corrections by the operators are required due the systematic variations of the process, such as the distortions generated in the joint preparation, resulting from the bevel machining or assemble of joint. These characteristics are translated in position problems, varying in the root opening, and in its concentricity and cylindricity, among other dimensional variations. These distortions affect welding process stability and torch positioning, which does not keep constant along the entire process, as discussed by Bae et al. [3].

There are various requirements associated with the need for innovation, most notably the following: the improvement of fusion welding processes, regarding the control and stability of metal transfer and energy supply; the development of techniques and equipment to minimize discontinuities; and increased productivity and repeatability, as detailed by Jeff [1] and Bae et al. [3]. In this regard, the cited authors mention that there is a demand for research on automated welding systems, specially to minimize the influence of the operator and aggregated inconsistencies over the welding process [4, 5].

Hongyaun et al. [6] and Chettibi et al. [7] emphasize that, in general, with the mechanization of processes there remains the need for significant human input, as the systems operate in “Teach and Play” routines, e.g., the operator defines positions and parameters (welding and movement) and the robot performs a blind operation in open loop, without any type of corrections. Thus, orbital welding operations that require real-time correction still need direct action by the operator/welder on the parameters (current, voltage, wire speed) and movement (welding speed, weaving, path) during the welding. To clarify the need to assist the welding operator in this task, for example, for a setup of 2.5 mm/s welding speed and 30 mm welding distance (this is the offset used between sensor and arc in this paper), a welder should be able to make manual corrections to all these parameters every 12 seconds, while the adaptive system used here operates at 25 Hz, meaning it acts on all these parameters every 0.04 seconds.

To make welding possible with full independence from the welder, it is necessary to emulate not only their manual skills and tacit knowledge about the process, but also the cognitive functions applied in the operation. These functionalities are the objective of the integrative technology called adaptive welding, which adds the use of sensors and mechatronic equipment with adequate geometric precision, repeatability, and robustness, as well as intelligent algorithms (strategies, routines, control, and correction algorithms).

Pires et al. [8, 9] describe sensing systems that can be used to track the joint and keep the torch focused on it during the welding, by means an adaptive control of the robot's movement. However, it has been observed that the effective use of complex joint-measuring sensors during the welding processes is relatively rare, being restricted to highly specific situations with high quality and low tolerance requirements.

Research has been developed to concatenate the communication between sensors and manipulators for welding applications. Rout et al. [10] published a review that details the main sensors used in the joint monitoring in welding processes and highlighted that sensor based on vision, in specific laser vision, are mostly efficient than others such as arc, touch, ultrasonic and others.

Vision sensors applied to the welding operation are mostly based on laser technology. The principle of optical triangulation of the laser sensors described by Kennedy [11] and Juneghan [12] consists of the projection of a light sheet, by means of a low power laser diode, generally with a power of less than 100 mW and with wavelengths close to infrared, on the surface to be measured.

With the information provided by the sensor, it is possible to develop complex systems of trajectory and parameter correction, which in practice considerably reduces the number of non-conforming parts, as shown by Pires et al. [8]. Thus, research has been aimed at the development of these systems. He et al. [13] described an automated system consisting of an anthropomorphic robot and a laser sensor, for multi-pass welding employing GMAW process. In addition, Hou et al. [14] presents a teaching-free welding method based on laser visual sensing system (LVSS) for robotic gas metal arc welding (GMAW). To verify the accuracy and robustness of the proposed method, experiments on V-grooves and fillet welds were performed. The results showed that the control accuracy on the V-groove and the fillet welds is suitable for most robot welding applications.

The measurement method based on laser triangulation is not limited to welding. However, it can be used in a wide range of applications. In welding, active sensors integrated with robotic manipulators are used for predetermining trajectories, measurements, and surface inspection, which are essential for adaptive control. Huang and Kovacevic [15] developed a system for weld inspection with an uncertainty of ± 0.55 mm. This system consists of three modules, a laser sensor, an image processing module, and a Cartesian motion control module. Li et al. [16] presents a Cartesian system for welding large-diameter tubes, where the arm has two degrees of freedom and carries a torch and the laser vision system in the effector. The tube is mounted on a rolling base that carries out the radial movement, where the welding torch is always in a flat position. This work presents methodologies for online joint tracking, i.e., during processing, which are validated using the submerged arc process.

Marmelo [17] presented a system for the adaptive orbital welding of narrow gap-type joints, using a laser triangulation sensor as a source of information to feed the algorithm developed. The system was composed of the integration of three main modules, a Serimax Saturnax 5 orbital welding manipulator, a Linconl welding source, using the GMAW-P synergic process, and a Mini-I/60 Robot Servo Laser sensor. The results reported show that the system was able to perform automatic welding and joint inspection. The algorithm uses equations developed from regression analysis of empirical tests.

In addition, Marmelo [17] highlighted the need for research on the automation of the pipeline welding process, as corroborated by Jeff [1], Shimon [4] and Chen [5]. However, there is little scientific information available on the practical implementation of this research in the industry.

Kindermann et al. [18] investigated the use of sensors for real-time correction in orbital welding, where an anthropomorphic robot was used to conduct the torch. The sensors for joint monitoring, such as: an arc sensor and a sensor based on electrical contact. Based on this hardware, algorithms to generate an automatic orbital trajectory and welding parameterization were developed. The proposed strategy and torch control by the arc sensor were validated by means of deposits on pipe specimens. The root pass welding was performed using the short-circuit controlled GMAW process together with the arc sensor. The main problem encountered was the need for constant oscillation of the welding torch as a function of the operational arc sensor characteristics.

This paper focuses on developing an AI-based on laser tracking system for root pass welding in pipes, utilizing a controlled short-circuiting GMAW technology (CCC). The study employed a dedicated 7-axis anthropomorphic robot integrated with a laser sensor. The first goal was to develop a robust integration between the robot and the laser sensor, enabling the creation of an online weld seam tracking algorithm to find and adjust the torch path along the welding of the joint. The second objective was to develop an intelligent algorithm able to use the real-time laser sensor data as input to parametrize the orbital welding procedures, in this study, only for root pass with opening of 0 to 4.5 mm.

## 2. MATERIALS AND METHODS

### 2.1 Real-Time Path Correction Algorithm

Initially, the communication and integration of the system components was carried out. The integration was made among Engemovi RES 7 4 780T, IMC A7 welding source and the Metavision SLS V1 laser triangulation sensor. All these equipment was integrated using ethernet protocol by means a property C# algorithm called adaptive welding platform (AWP). In this setup the laser sensor was positioned 30 mm in front of the torch, in order to avoid the arc noise, following the manufacturer's recommendations. This distance between the laser line and the torch was called ‘offset’. The experimental setup used is shown in Figure 1.

The algorithm developed is constantly fed with information coming from the manipulator and laser sensor at a rate of 25 Hz. The manipulator provides TCP (tool center point) data position (X, Y and Z) for every millimeter traveled by the welding torch (TCP) on the rail (X). The laser sensor provides information of the joint geometry, where the root gap is the main parameter of interest. In addition, the laser sensor provides relative position of a defined tracking point (TP), in this case defined as the center of the joint. To find out the torch deviation the AWP algorithm calculates the difference between of the laser and torch Y and Z for each respective X coordinate position.

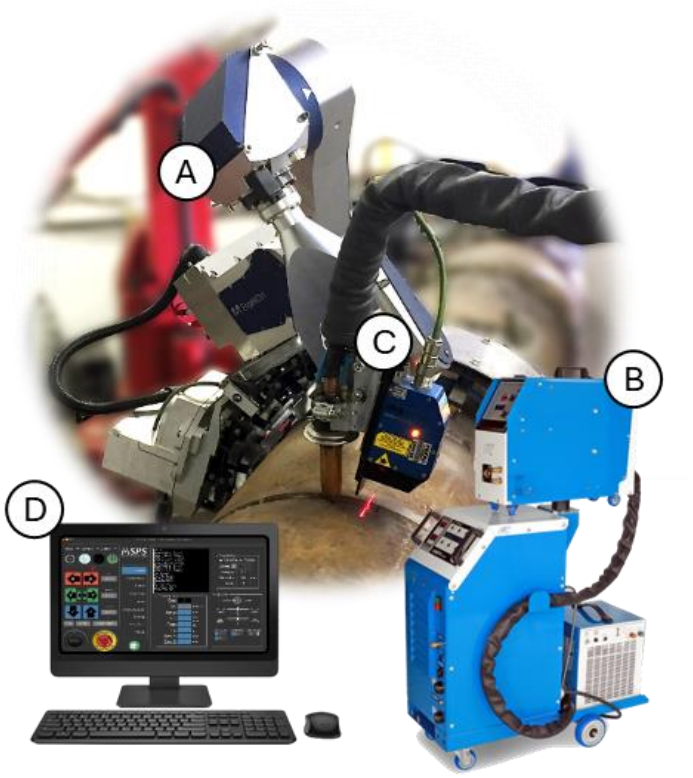


**FIGURE 1:** SCHEMATIC SETUP OF THE ADAPTIVE WELDING SYSTEM, WHERE: A) ENGEMOVI RES 7 4 780T 7-AXIS ROBOT ON RAIL; B) IMC A7 DIGIPLUS WELDING POWER SOURCE; C) METAVISION SLS V1 LASER SENSOR; D) AWP;

As previously described, given the need for a lag between the laser sensor and the welding torch due to the influence of the electric arc, a 30 mm displacement of the torch in relation to the laser sensor was used. This layout required previous scanning of the region between the laser sensor and the torch, which is referred as the offset. Initially the manipulator moves 30 mm in the opposite direction to the welding (exactly the offset value), the region is scanned until the offset is zero and the corrected path is executed. The scheme in Figure 2 illustrates the offset reading procedure. This previous scan stores information related to TP and TCP in a buffer, as well as information on the correction to be applied (point by point).

The AWP algorithm receives for each X position the Y and Z coordinates from both the TCP and TP, with TCP position being informed by the manipulator and the TP by the laser sensor. The sum of these points (TCP and TP position) results in a point that represents the correct TCP position on the TP (joint center). These points represent the path that must be executed by the torch to maintain the TCP over the TP, i.e., the joint trajectory correction map. Due to the difference in sensor acquisition frequency and manipulator weaving frequency, Y Path values/Y position values read oscillate around a mean

curve. To attenuate this noise, a low-pass filter (exponential smoothing) is used, which smoothes the reading of the manipulator movement.

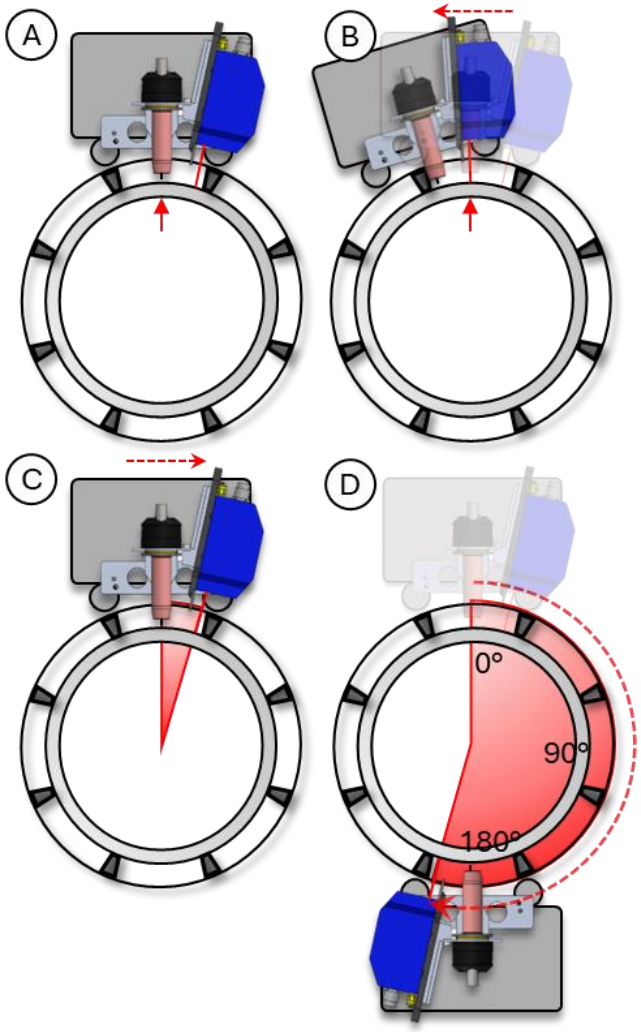


**FIGURE 2:** SCHEMATIC EXAMPLE OF OFFSET SCANNING: A) TORCH ON TCP IN P0; B) MANIPULATOR BACKWARD; C) OFFSET SCANNING AND BUFFER FILL; D) PROCESS EXECUTION.

Additionally, as described by Chen et al. [19], Yang et al. [20], and Hou et al. [14], before the welding procedures, an initial calibration of the system is required to map the shape error present on the rail due to the mobile base and the relation between the robot rail and pipe shape, Figure 3 illustrates such effect due to the systematic error.

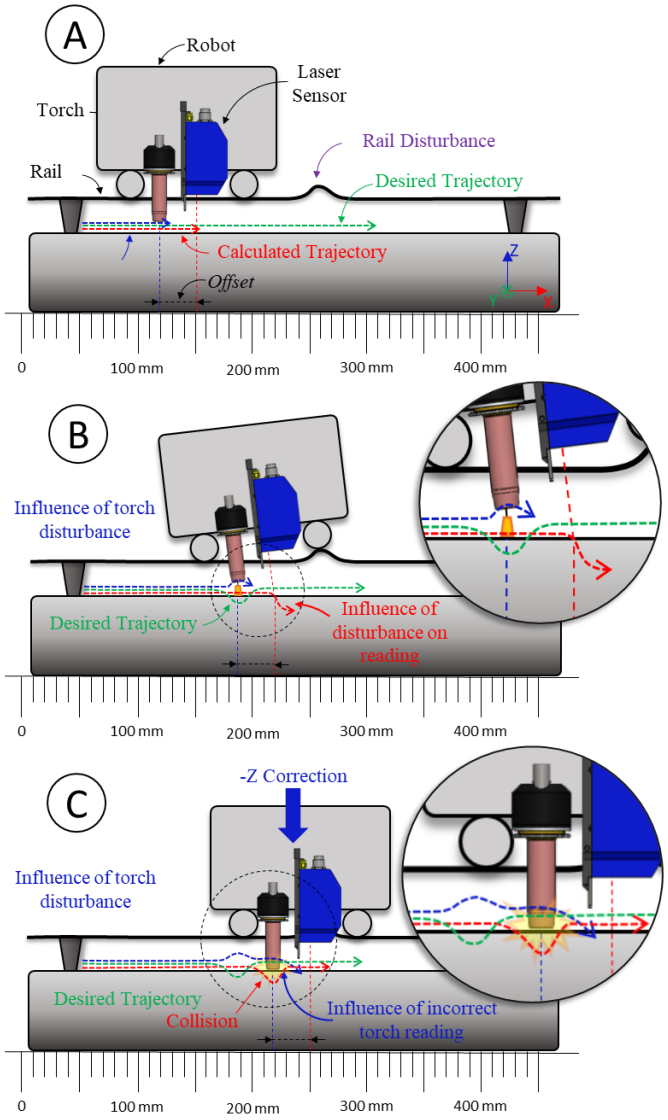


**FIGURE 3:** REPRESENTATION OF THE SHAPE ERROR AS A FUNCTION OF THE OFFSET ON THE PATH, WHERE: A) SYSTEM IN UNDISTURBED MODE; B) DISTURBANCE IN THE PATH GENERATED BY A SHAPE ERROR ON THE RAIL; AND C) RETROACTIVE EFFECT ON THE PATH DUE TO THE SHAPE ERROR ON THE RAIL.

In this context, to mitigate systematic errors resulting from the deviation due to the relation between the pipe shape and the robot rail, a preliminary joint scan is performed using the laser at the TCP, seeming the joint under a view of torch perspective, after that another joint scan with torch in the original position (TCP) is performed. The difference between these X, Y and Z points represents the rail correction which must be add in real-time correction during the process execution. This step is referred to as rail calibration. These steps are represented in 4.

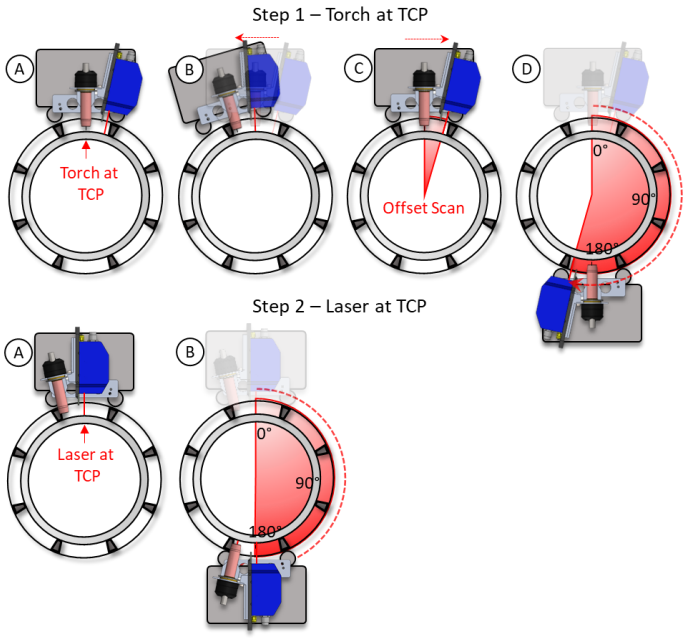


**FIGURE 4:** FLOWCHART OF THE ADAPTIVE WELDING PROCESS DEVELOPED, WHERE STEP 1: A) TORCH POSITIONING AT PART ZERO; B) BACK OF THE SYSTEM FOR OFFSET COMPENSATION; C) READING THE OFFSET; D) SCANNING THE JOINT; AND STEP 2: A) LASER AT TCP (SAME POSITION AS THE TORCH); B) JOINT SCAN FROM TORCH PERSPECTIVE.

### 2.3 Adaptive welding algorithm based on discrete AI.

The second part of the present study was the adaptive welding platform (AWP) algorithm, this algorithm was based on an AI methodology for parametrize the welding process in real-time using as input the joint gap (measured by laser) and torch position (robot output). Initially, the joint type was defined, in this case was the V-type groove with 30° bevel without noise and operationally gap range was defined in 0 to 4.5 mm. The wire feed and procedure gas used were the 1.2 mm wire steel ER70S6 and C25 (75% Argon and 25% $CO_2$). The welding process used consists of a GMAW variant, i.e. a controlled short-circuit (CCC) that offers high stability and robustness to the process allowing greater control out of position and with large root gaps. This GMAW version is based on surface tension metallic transfer, that is, presents low spatter and fumes emissions.

Two waveforms were used, that is, high and low heat input. For gaps with 0 to 1 mm an average current of 150 A was used and for gaps from 2.5 to 4.5 mm an average current of 100 A was used, based on the Silva and Dutra [21] work. However, for root opening between 1.0 and 2.5 mm a linear interpolation was used between the average current that refers to the gap of 1 mm (150 A) and that for 2.5 mm (100 A). It should be noted that this process is based on a conventional short-circuiting, however controlled by the current. For a better understanding of the controlled short-circuit process used the reader is referred to the work of previous authors. Figure 5 shows the general aspect of this controlled short-circuit waveform version. Aiming to establish stable welding parameterization that is appropriate for the root opening range previously stipulated, two welding waveforms were defined, one with a higher (150A) and one with a lower (100A) mean current, in order to maintain a margin of tolerance and increase the robustness of the system.

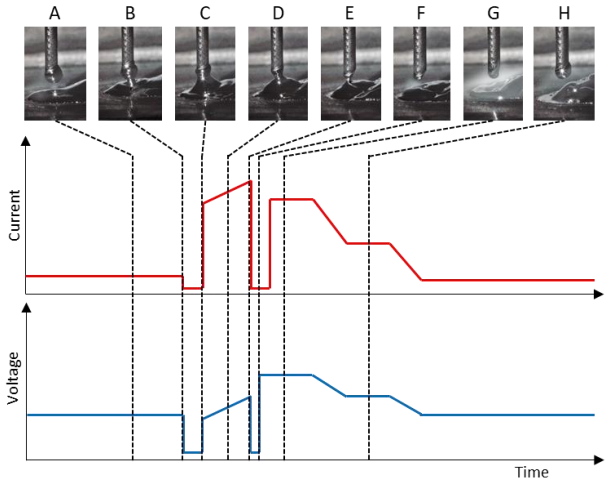


**FIGURE 5:** GENERAL ASPECT OF THE TYPICAL CURRENT AND VOLTAGE WAVEFORM FOR GMAW-CCC SHORT-CIRCUIT CONTROLLED

In order to feed the AWP database, parametrization tests were performed on samples made of 300 x 100 x 12.7 mm ASTM A36 steel sheets. In these tests were defined the torch movement parameters (amplitude, oscillation frequency, stop time and welding speed) and the Controlled short-circuit GMAW welding parameters. The welds were carried out at positions that describe 180° of a tube, i.e., flat, vertical-down and overhead position. In total, 27 tests were performed, with 3 valid specimens extracted by root gap and position. All the parametrization tests were carried out in the RES 7 anthropomorphic robot.

A set of variables was sought that results in a certain geometric pattern of the weld root, considering a single V-groove joint with 30° bevel. The acceptance criteria for qualifying the root pass were defined, as follows:

1. Root concavity: ≤ 0.05 t and maximum 0.5 mm, where t is the wall thickness. According to ISO 5817 [22] (quality level B).
2. Root reinforcement: ≤ 1 mm + 0.2 b and maximum 3.0 mm, where b is the width of the root. According to ISO 5817 [22] (quality level B).
3. Convexity or concavity on the face: Although there is no specific recommendation in this regard for the root pass, a maximum value of 1.5 mm in height was considered. This value refers to the finishing pass, according to the ASME IX standard [23].
4. Surface defects, such as cracks, bites, and lack of fusion, according to API 1104 [24].

Therefore, the AI adaptive algorithm methods related to each welding variable mentioned above to the root gap and angular position using regression methods, similar to the methods presented by Yan et al. [25]. The output data is basically the welding parameters (amplitude, oscillation frequency, stop time and welding speed) and the controlled short-circuit GMAW waveform (Higher or Lower mean current)

Finally, validation tests were performed to both the joint tracking and the adaptive parameterization algorithm. In these tests, circular specimens made from API 5L grade B steel pipe segments with 16” diameter and 3/8” thickness were welded in the 5G position, with the aforementioned single V-groove with 30° bevel. In addition, a variable root opening between 1 mm and 4.5 mm was used. the Figure 6 shown the experimental setup used in the final welding tests.


**FIGURE 6:** EXPERIMENTAL SETUP USED IN THE VALIDATION TESTS.

## 3. RESULTS AND DISCUSSION

The root macrographs of the specimens obtained for each root opening and position are illustrated in Figure 7. Each sample was evaluated according to the proposed methodology using the cited standards. As can be seen, the results indicate the absence of defects, with good dilution and adequate penetration. It should be noted that five repetitions were performed per set of parameters to verify repeatability.

The samples in the vertical-down position exhibited a slight concavity at the root. However, as depicted in Figure 7, complete fusion of the edges and the root was observed, indicating total penetration in accordance with API 1104 standards.

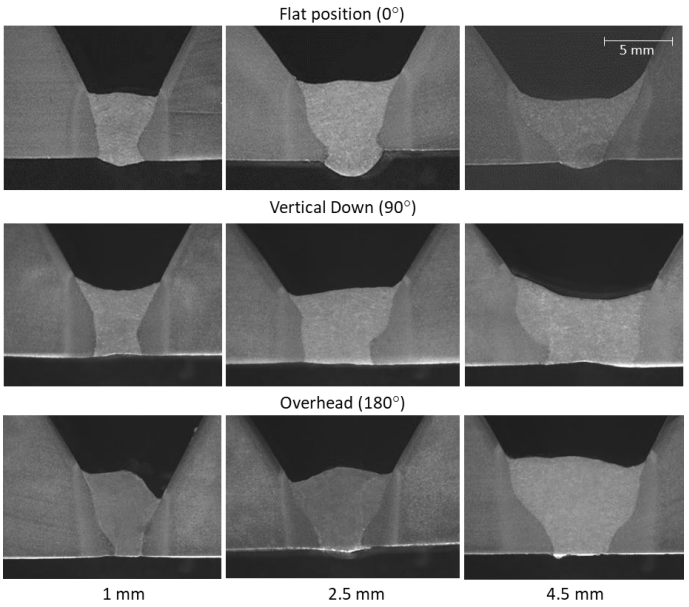


**FIGURE 7:** MACROGRAPHY OF THE ROOT PASSES SPECIMENS USED TO PARAMETERIZE THE ADAPTIVE ALGORITHM

The empirical data obtained and defined as suitable for the sample welding on plate in flat, vertical-down and overhead position were used as base for the AWP parameterization. The data obtained, i.e., amplitude, oscillation frequency, idle time or stop time, and travel speed were used in the regression analysis in function of root opening to model mathematically the behavior of each cited component and position. This part of the work provides enable the AI capability of adapt the process due to the variation at the root opening. The data obtained can be seen in Table 1.

**TABLE 1:** WELDING PARAMETERS OBTAINED IN THE BEST SAMPLE RESULTS.

| Position | RG | Amp. | Freq. | ST | TS | I | WFS |
|---|---|---|---|---|---|---|---|
| Flat | 1.0 | 0 | 0 | 0 | 30 | 150 | 5.0 |
| | 2.5 | 2.8 | 0.8 | 0.4 | 12 | 100 | 3.2 |
| | 4.5 | 7 | 0.7 | 0.3 | 8 | 100 | 3.2 |
| Vertical | 1.0 | 0 | 0 | 0 | 35 | 150 | 5.0 |
| | 2.5 | 3 | 0.6 | 0.3 | 14 | 100 | 3.2 |
| | 4.5 | 6 | 0.6 | 0.3 | 8 | 100 | 3.2 |
| Overhead | 1.0 | 0 | 0 | 0 | 30 | 150 | 5.0 |
| | 2.5 | 3 | 0.8 | 0.3 | 12 | 100 | 3.2 |
| | 4.5 | 6 | 0.6 | 0.3 | 7 | 100 | 3.2 |

From the regression analysis, the function with the highest R-square value was selected for each parameter. The following functions were obtained to mathematically describe the behavior of each parameter as a function of the gap or root opening. The function obtained can be seen in Table 2. It was observed that each parameter exhibits a distinct behavior. For example, amplitude displayed a linear pattern, frequency

exhibited logarithmic behavior similar to stop time, and travel speed demonstrated a potential behavior. Additionally, it was observed that each parameter was influenced by the welding position. This behavior occurs due to the dynamic changes in metallic transfer, which vary for each position.

**TABLE 2:** MATHEMATICAL REPRESENTATION AS A FUNCTION OF THE GAP FOR EACH WELDING PARAMETER COMPONENT

| | Flat | Vertical-down | Overhead |
|---|---|---|---|
| Amp. | f(x) = 2.01 x - 2.08 | f(x) = 1.70 x - 1.54 | f(x) = 1.70x - 1.54 |
| Freq. | f(x) = 0.5 ln(x) + 0.1 | f(x) = 0.42 ln(x) + 0.06 | f(x) = 0.44 ln(x) + 0.11 |
| ST | f(x) = 0.15 ln(x) + 0.15 | f(x) = 0.21 ln(x) + 0.03 | f(x) = 0.21 ln(x) + 0.03 |
| TS | $f(x) = 29.16\ x^{-0.89}$ | $f(x) = 29.16\ x^{-0.89}$ | $f(x) = 29.77\ x^{-0.97}$ |

In order to mitigate the probability of defects resulting from abrupt parameter changes in transient regions, such as the midpoint (45°) between the flat and vertical-down positions, which was not explored, the AI algorithm applies a linear regression between the parameters for the instantaneous gap for the position between both, e.g., the position 45°, the resulting parameters are defined as 50% of each position, flat and vertical, for position 72°, e.g., the resulting parameters are defined as 80% of vertical and 20% of flat position. The same procedure was followed for the intermediate points between the vertical-down and overhead positions. Additionally, the same strategy was applied for the welding current and WFS, however, only for the gaps between 1 and 2 mm, representing the transition from high to low welding energy, as described in the methodology.

This strategy considers the positional changes along the pipe circumference, with the set increment being one degree. This means that the parameters are corrected for each degree.

In the validation tests, tubular specimens with V-joint forementioned. These tests demonstrated that the AI adaptive algorithm (joint tracking + parameter corrections) correctly adjusted the welding torch path and welding parameters online in real-time. The path correction algorithm showed effective behavior towards joint mismatch, as depicted in Figure 8, which illustrates the mismatch errors in Y and Z as a function of angular position (X). Therefore, the corrections made on the pipe joint using the developed methodology exhibited great performance and robustness, allowing for the identification and adjustment of the TCP to mitigate positional errors.

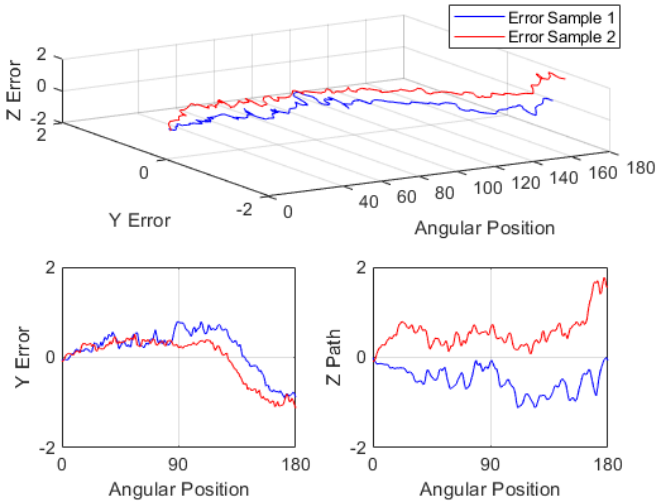


**FIGURE 8:** MISMATCH ERRORS IN Y (TORCH OSCILLATION) AND Z (CTWD) ALONG THE TORCH PATH AROUND THE JOINT

The adaptive algorithm shown an effective behavior in function of the gap, correcting the weaving (amplitude and oscillation frequency), welding speed and welding parameters (current and wire feed speed) in real-time. Even so, the joints remained within the previously established criteria, with root openings from 1.0 to 4.5 mm. The graph in Figure 9 illustrates the root opening varying along the torch path around the pipe joint. In the 0° region of the anti-clockwise joints an opening of about 7.5 mm can be observed, which represents the beginning of the previous bead, that is, its overlap.

It was found that in certain instances along the section, the error resulting from the deviation in the Y path exceeded 85% of the root opening. For example, in the 80° region of SP1, without compensation, a serious welding defect could occur, such as burn-through or insufficient penetration. The same applies to the compensation of the Z error, which can lead to variations in the average voltage and may suggest a change in the position of wire insertion over the weld pool, thereby altering the previously calibrated TCP. However, both parts of the AWP AI algorithm for pipe welding shown a good performance towards all conditions analyzed in the final tests.

The face and root appearance of the welded specimens are shown in Figure 10 and Figure 11, with four repetitions performed on two complete tubular joints. It's worth noting that the welds were consistently made from the flat position to the overhead position.

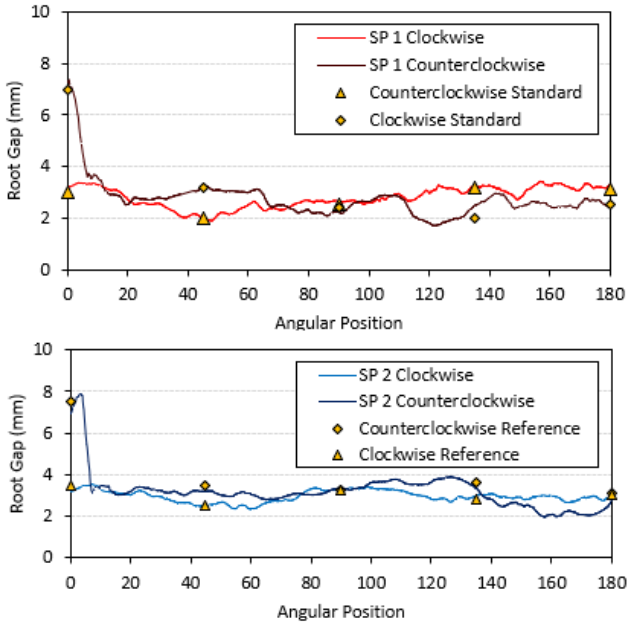


**FIGURE 9:** ROOT OPENING VARYING MEASURED BY THE LASER SENSOR

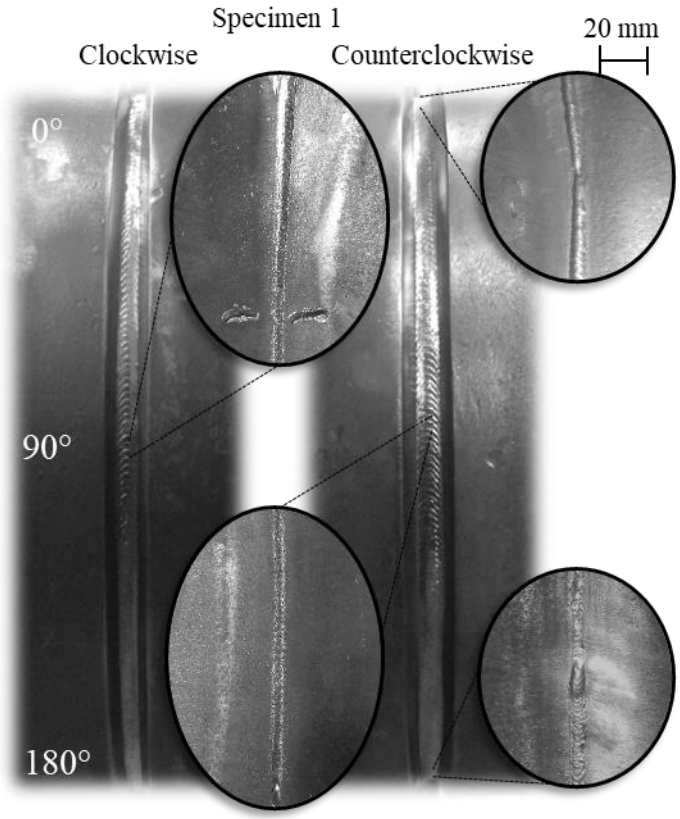


**FIGURE 10:** RESULTS OBTAINED FOR SAMPLE 1 USING THE AI ADAPTIVE ORBITAL WELDING ALGORITHM (WHEN PRESENT, TRANSVERSAL MARKS ASIDE THE ROOT (BOTTOM) VIEW WELDS ARE NOT A WELD DEFECT, HOWEVER MARKS OF THE C ASSEMBLY FIXING ACCESSORY).

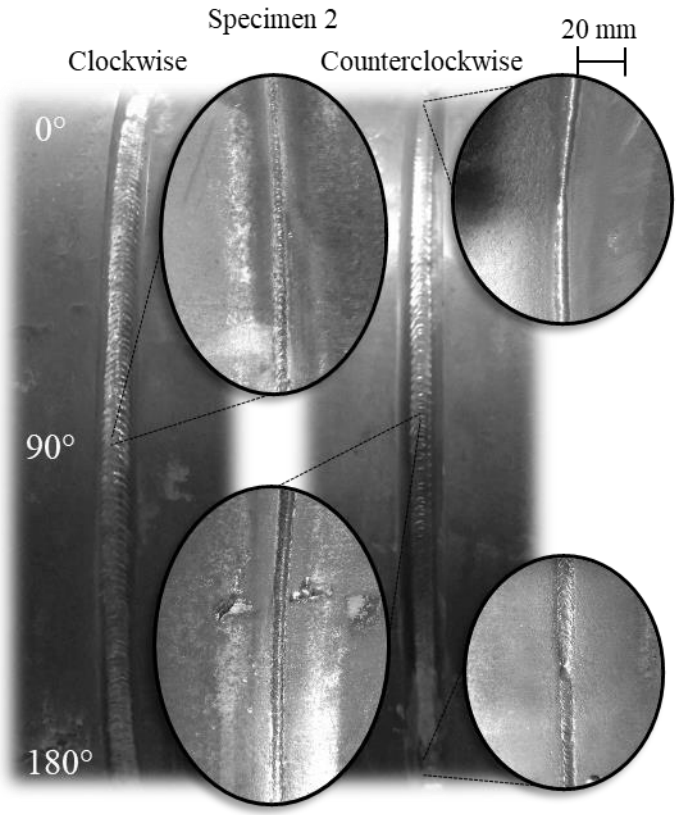


**FIGURE 11:** RESULTS OBTAINED FOR SAMPLE 2 USING THE AI ADAPTIVE ORBITAL WELDING ALGORITHM (WHEN PRESENT, TRANSVERSAL MARKS ASIDE THE ROOT (BOTTOM) VIEW WELDS ARE NOT A WELD DEFECT, HOWEVER MARKS OF THE C ASSEMBLY FIXING ACCESSORY).

The criteria described in the methodology were used for the qualification of the root passes made in the specimens. For the concavity limit the maximum value was -0.5 mm and for the reinforcement the root width ratio was used for 5 quadrants along the pipe, according to ISO 5817. Table 3 reports the reference limits calculated using the cited standard.

**TABLE 3:** REFERENCE LIMITS FOR THE ROOT REINFORCEMENT (mm).

| | SP 1 | | SP 2 | |
|---|---|---|---|---|
| Position | CW | CCW | CW | CCW |
| 0° | 2.2 | 2.2 | 2.2 | 2.2 |
| 45° | 1.9 | 2 | 2.2 | 2 |
| 90° | 2.2 | 1.6 | 2 | 2 |
| 135° | 2 | 1.9 | 2 | 2 |
| 180° | 2 | 2 | 2.4 | 2.4 |

The results of the measurements for the five quadrants are given in Table 4. In the case of the concavity, it can be observed that all quadrants adhered to the limit of -0.5 mm. For the reinforcement, taking into consideration the relation with

the root width in each quadrant, it can be observed that all measurements were within the established limit values. Taking the welded specimen results in consideration, the developed system showed potential for field operations, especially for large diameter pipes joining operations.

**TABLE 4:** ROOT REINFORCEMENT AND CONCAVITY MEASURES (mm).

| | SP 1 | | SP 2 | |
|---|---|---|---|---|
| Position | CW | CCW | CW | CCW |
| 0° | 0 | 0 | 2 | 2 |
| 45° | 1.5 | 1.8 | 2.5 | 2 |
| 90° | 0 | 0 | 0 | 0 |
| 135° | -0.2 | 0 | 0 | -0.2 |
| 180° | -0.4 | -0.4 | -0.2 | -0.2 |

## 4. CONCLUSION

The system developed in this work, as well as the proposed AI algorithms (for seam tracking and adaptive welding) performed as expected, both theoretically and experimentally.

The algorithm for path correction and rail calibration demonstrated its usefulness in situations where the manipulator is installed over the weld specimen. In this case, it is common for its rail to deform, resulting in random torch movement during welding if these distortions are not compensated. The proposed algorithm may also be used for rail calibration of welding cells upon installation, consisting of an algorithm with full capability of delivering a good result for this task also. Welding inspection apparel that uses rails or the base metal as its track can also benefit from the proposed algorithm for the offset/rail/base calibration. As a previous scan was implemented in order to calibrate the rail deformation, this algorithm allows single laser line projection sensors to be utilized for this functionality. Despite adding one more step, rail calibration improves the overall quality and productivity of welding and pipe construction, due to the increased robustness and reliability of the automatic welding process (adaptive welding).

The AI adaptive welding algorithm developed also showed promising results, being able to adapt the parameters for the gap variations presented within the range of groove geometry variability and pipe mismatch. The methods also have the potential to be applied in the metal-mechanical industry in general due to the ability to improve automated welding, and so not restricted for large pipe diameter welding applications.

These algorithms can be used in further developments, for example, on the development of filling pass strategies in next works.

It is worth noting that all these experiments were limited to laboratory tests and shop fabrication. However, in future work, there is potential to adapt and apply that system in specific tests for pipeline construction.


## ACKNOWLEDGEMENTS

The research proposed in this paper was supported by Labsolda - Mechatronic and Welding Institute, Federal University of Santa Catarina, IMC and Petrobras.


## REFERENCES


[1] Jeff N (2013) Maximizing pipeline welding efficiency. Welding Journal. Miami, Florida. 92(6):74-78. ISSN 0043-2296.

[2] Marques PV, Modenesi PJ, Bracarense AQ (2009) SOLDAGEM – Fundamentos e Tecnologia. UFMG, Brazil.

[3] Bae KY, Lee TH, Ahn KC (2002) An optical sensing system for seam tracking and weld pool control in gas metal arc welding of steel pipe. Journal of Materials Processing Technology 120(1-3):458 – 465. Https://doi.org/10.1016/S0924-0136(01)01216-X

[4] Shimon Y (1999) Handbook of Industrial Robotics. New York.

[5] Chen S (2003) On intelligentized technologies for modern welding manufacturing. Chin. J. Mech. Eng. 16(4):367–370.
Https://doi.org/10.3901/CJME.2003.04.367

[6] Hongyuan S, Xixia H, Tao L, et al. (2009) Weld formation control for arc welding robot. Int J Adv Manuf Technol 44:512–519. Https://doi.org/10.1007/s00170-008-1847-0

[7] Chettibi T, Lehtihet HE, Haddad M, Hanchi S (2004) Minimum cost trajectory planning for industrial robots. Eur. J. Mech. 23(4):703–715. https://doi.org/10.1016/j.euromechsol.2004.02.006

[8] Pires JN, Loureiro A, Bölmsjo G (2006) Welding Robots: Technology, System Issues and Application. Springer Science & Business Media. London. https://doi.org/10.1007/1-84628-191-1

[9] Pires JN, Bolmsjö G, Olsson M (2005) Sensors in robotic arc welding to support small series production. Ind. Robot 32(4):341–345.
https://doi.org/10.1108/01439910510600218

[10] Rout A, Deepak BBVL, Biswal BB (2019) Advances in weld seam tracking techniques for robotic welding: A review. Robotics and Computer Integrated Manufacturing, 56:12-37.
https://doi.org/10.1016/j.rcim.2018.08.003

[11] Kennedy WP (2017) The Basics of Triangulation Sensors.Available:http://archives.sensorsmag.com/articles/0598/tri0598/. Accessed 23 November 2017.

[12] Juneghani B, Noruk J (2009) Keeping Welding Costs from Spiraling Out of Control. The Fabricator (1):42 - 44.

[13] He Y, Xu Y, Chen Y, Chen H, Chen S (2016) Weld seam profile detection and Feature point extraction for multi-pass route planning based on visual attention model. Robotics and Computer-Integrated Manufacturing. 37:251-261. https://doi.org/10.1016/j.rcim.2015.04.005

[14] Hou Z, Xu Y, Xiao R, Chen S (2020) A teaching-free welding method based on laser visual sensing system in robotic GMAW. Int J Adv Manuf Technol 109:1755–1774. https://doi.org/10.1007/s00170-020-05774-0

[15] Huang W, Kovacevic R (2012) Development of a real-time laser-based machine vision system to monitor and control welding processes. Int J Adv Manuf Technol. 63:235-248. https://doi.org/10.1007/s00170-012-3902-0

[16] Li Y, Xu D, Yan Z, Tan M (2007) Girth Seam Tracking System Based on Vision for Pipe Welding Robot. In: Tarn TJ., Chen SB., Zhou C. (eds) Robotic Welding, Intelligence and Automation. Lecture Notes in Control and Information Sciences. 362:391-399. https://doi.org/10.1007/978-3-540-73374-4_47

[17] Marmelo PC (2012) Real Time Evaluation of Weld Quality in Narrow Graoove Pipe Welding. Phd Thesis. Cranfield University.

[18] Kindermann RM, Silva RHG, Dutra JC (2015) Development and Validation of Algorithms Employed for Sensor Systems in Robotic Orbital Root Pass Welding of Pipelines. International Welding. 20(4):391-402. https://doi.org/10.1590/0104-9224/SI2003.08

[19] Chen X, Dharmawan AG, Foong S, Song Soh GS (2018) Seam tracking of large pipe structures for an agile robotic welding system mounted on scaffold structures. Robotics and Computer–Integrated Manufacturing. 50:242-255. https://doi.org/10.1016/j.rcim.2017.09.018

[20] Yang L, Liu Y, Peng J, Liang Z (2020) A novel system for off-line 3D seam extraction and path planning based on point cloud segmentation for arc welding robot. Robotics and Computer Integrated Manufacturing. 64:1-14. https://doi.org/10.1016/j.rcim.2019.101929

[21] Silva RHG, Dutra JC (2009) Controlled short-circuit GMAW welding (CCC) - Processing analysis Tools. Welding and Cutting, 8(3):162-167.

[22] The International Organization for Standardization. ISO 5817: Welding - Fusion-Welded joints in steel, nickel, titanium and their alloys (beam welding exclued) - Quality levels for imperfections (2003) International Standard: Switzerland. [S.l.].

[23] American Society of Mechanical Engineers. ASME IX: Qualifications Standard for Welding, Brazing and Fusing Operators (2015) The American Society of Mechanical Engineers. New York.

[24] API Standard 1104 - Welding of Pipelines and Related Facilities (2013) American Petroleum Institute. [S.l.], 21:118.

[25] Yan M, Zhang K, Liu D, Yang H, Li Z (2020) Autonomous programming and adaptive filling of lap joint based on three-dimensional welding-seam model by laser scanning. Journal of Manufacturing Process, 53:396-405. https://doi.org/10.1016/j.jmapro.2020.03.034